DOI: 10.1002/ejic.201000741

MMX Chains and Molecular Species Containing Rh_2^{n+} (n = 4, 5, and 6) Units: Electrical Conductivity in Crystal Phase of MMX Polymers

Pilar Amo-Ochoa,[a] Reyes Jiménez-Aparicio,*[a] M. Rosario Torres,[b] Francisco A. Urbanos,[a] A. Gallego,[c] and Carlos J. Gómez-García[d]

Keywords: Rhodium / Polymers / Conducting materials / Metal-metal interactions / Molecular wires / Electrical properties / Metal-organic frameworks / Paddlewheel compounds

The control of the experimental conditions in the reaction of $Rh_2(O_2CCH_3)_4$ with halides allows the isolation of the novel dirhodium complexes $K_x[Rh_2X(O_2CCH_3)_4]_x \cdot 4xH_2O$ (X = Br, **1·4H$_2$O** and I, **2·4H$_2$O**) $[Rh_2(O_2CCH_3)_4Cl]_x \cdot xH_2O$ (**3·H$_2$O**), $[Rh_2(O_2CCH_3)Cl]_x \cdot 4xH_2O$ (**3·4H$_2$O**), and $[Rh_2(O_2CCH_3)_4I_2] \cdot 4H_2O$ (**4·4H$_2$O**) containing Rh_2^{n+} (n = 4, 5 and 6) units. The X-ray structure determination of compounds **1**–**4** reveals the presence of dirhodium units in different oxidation states. The polyanionic complexes **1·4H$_2$O** and **2·4H$_2$O** containing Rh_2^{4+} units give *zig-zag* chains. In contrast, the partially oxidized complexes **3·H$_2$O** and **3·4H$_2$O** containing Rh_2^{5+} units are linked by chloride ligands forming linear chains. The first tetracarboxylatodirhodium(III) compound **4·4H$_2$O** is also described. Its structure consists of discrete binuclear $[Rh_2(O_2CCH_3)_4]^{2+}$ units with both axial positions occupied by iodide ligands. The very simple synthetic procedures presented here to achieve the partial or complete oxidation of the dirhodium(II) precursors open new perspectives in dirhodium complexes containing different oxidation states and in their potential applications in the construction of molecular devices. The electrical characterization of the polymer chains confirms conductivity in crystal phase. In addition, isolation of **1·4H$_2$O** and **2·4H$_2$O** on mica and morphological characterization of individual chains by atomic-force microscopy have been achieved.

Introduction

Since the discovery of metal–metal multiple bonds, the study of dimetallic compounds has occupied a central role in transition-metal chemistry.[1] The theoretical aspects of the metal–metal bond and the applications of this type of complexes in several fields are the main causes of their rapid development.[1] In this regard, research involving dirhodium complexes is also a matter of interest. The properties of these compounds span diverse fields such as molecular architecture, catalysis, or antitumor activity, leading to an exponential growth of dirhodium chemistry.[2] Dirhodium carboxylates containing a Rh_2^{4+} core constitute the largest group of dirhodium(II) complexes with metal–metal bonds.[1,2] Oxidation reactions of these compounds to complexes with Rh_2^{5+} and Rh_2^{6+} cores are very difficult. Thus, the number of dirhodium complexes with mixed oxidation states, Rh_2(II,III), is scarce although some dirhodium complexes of the type $[Rh_2(L)_4]^+$ with different anionic bridging ligands (L) have been described.[1,3] The dirhodium(III) compounds are very scarce. To the best of our knowledge, only two types of dirhodium(III) complexes have been reported: a series of bis(phenyl)dirhodium(III) complexes,[4] and the $[Rh_2(O_2CR)_4(NO)_2]$ (R = Me, Et, *i*Pr) compounds,[5] but in the latter, the specific oxidation state is unclear. In addition, the required reaction conditions are too specific, for instance, the bis(σ-aryl)dirhodium(III) caprolactamates were obtained by reaction of bis(σ-aryl)dirhodium(II) caprolactamates with arylboronic acids in the presence of copper as a catalyst,[4c] and the $[Rh_2(O_2CR)_4(NO)_2]$ (R = Me, Et, *i*Pr) complexes were prepared by reaction of NO(g) with $[Rh_2(O_2CR)_4]$ under N_2.[5]

The use of dimetallic subunits has recently gained renewed attention due to the discovery of the fact that one-dimensional mixed-valence olygomers and polymers formed using these dimetallic building-blocks may generate compounds with novel applications, for instance, as molecular wires.[6–8] The complex $[Rh_4(1,3\text{-diisocyanopropane})_8Cl]^{5+}$ represented the first structurally characterized chain based

[a] Departamento de Química Inorgánica, Facultad de Ciencias Químicas, Universidad Complutense de Madrid, Ciudad Universitaria,
28040 Madrid, Spain
Fax: +34-1-3944352
E-mail: reyesja@quim.ucm.es
[b] Centro de asistencia a la investigación de rayos X, Facultad de Ciencias Químicas, Universidad Complutense de Madrid,
Ciudad Universitaria,
28040 Madrid, Spain
Fax: +34-1-3944352
[c] Facultad de Ciencias
Universidad Autónoma de Madrid, Campus de Cantoblanco
28049 Madrid, Spain
Fax: +34-1-4974833
[d] Instituto de Ciencia Molecular, Universidad de Valencia,
Parque Científico, 46980 Paterna, Spain
Fax: +34-963543273
Supporting information for this article is available on the WWW under http://dx.doi.org/10.1002/ejic.201000741.

on the Rh^{I}–Rh^{II}–Rh^{II}–Rh^{I} unit used with this objective.[9–11] Subsequently, some examples of oligomeric mixed-valence complexes with rhodium[1,12,13] and with other transition metal-ions have been prepared. New developments in this area include the preparation of analogous tetranuclear rhodium and iridium blues with catalytic properties.[14]

Other interesting one-dimensional polymers are those called MMX chains. In particular, $[Pt_2(dta)_4I]$ (dta = dithioacetate) presents exceptionally high electrical conductivity at room temperature in the crystal phase.[15–17] More recently, it has been reported that nanostructures of $[Pt_2(dta)_4I]$ on surface show high electrical conductivity.[18] These results have opened new perspectives towards the applications of these molecular wires in nanoelectronics.

However, the study of the electrical properties of MMX chains with other metals and ligands is still poorly developed. We have selected dirhodium compounds as an alternative based on the preliminary electrical measurements on halotetraacetamidatedirhodium(II,III) complexes[19–21] and the ability of rhodium atoms to form dimetallic cores bridged by carboxylate ligands. Moreover, carboxylate ligands are more stable than the dithiocarboxylates used in the conducting MMX platinum chains. Therefore, the use of carboxylates could lead to an increase of the functionality along the terminal ligands of the polymer chains (e.g. with H-bond donor-acceptor capabilities). In this paper we describe the synthesis of the first polymeric tetracarboxylatodirhodium(II) compounds $K_x[Rh_2X(O_2CCH_3)_4]_x{\cdot}4xH_2O$ (X = Br, **1·4H$_2$O** and I, **2·4H$_2$O**) and dirhodium(II,III) derivatives $[Rh_2(O_2CCH_3)_4Cl]_x{\cdot}xH_2O$ (**3·H$_2$O**) $[Rh_2(O_2CCH_3)_4Cl]_x{\cdot}4xH_2O$ (**3·4H$_2$O**). The preparation of the first tetracarboxylatodirhodium(III) complex $[Rh_2(O_2CCH_3)_4I_2]{\cdot}4H_2O$ (**4·4H$_2$O**) is also reported. Electrical characterization and preliminary studies on surfaces have been carried out in order to prove the application of these linear conductive chains as molecular wires.[22–24]

Results and Discussion

The reaction of tetraacetatodirhodium(II) and a potassium halide KX (X = Cl, Br, I) using water as a solvent leads to the formation of complexes **1**–**4**. These reactions were carried out under one of the following conditions:

a) Neutral solution without addition of oxygen.

b) Acid solution (HBF_4) saturated with oxygen.

c) Neutral solution saturated with oxygen.

Polymeric complexes $K_x[Rh_2X(O_2CCH_3)_4]_x{\cdot}4xH_2O$ (X = Br, **1·4H$_2$O** and I, **2·4H$_2$O**) and $K_2[Rh_2(O_2CCH_3)_4Cl_2]$ have been obtained using the procedure *a*. Under these conditions the oxidation of rhodium(II) is not observed.

However, the Rh_2^{4+} unit is partially oxidized to Rh_2^{5+} core in acid solution (HBF_4) saturated with oxygen (procedure *b*) in the presence of KCl and KBr giving the polymeric mixed-valence $[Rh_2(O_2CCH_3)_4Cl]_x{\cdot}xH_2O$ (**3·H$_2$O**), and $RhBr_3$, respectively. Complex **3·H$_2$O** was obtained in a very low yield (4%). In an attempt to prepare **3·H$_2$O** in a higher yield the similar oxidation reaction using NH_4Cl and $CuCl_2$ instead HBF_4 was carried out. In these new conditions a yield of 10% of the complex $[Rh_2(O_2CCH_3)_4Cl]_x{\cdot}4xH_2O$ (**3·4H$_2$O**) was achieved.

The addition of HX (Cl, Br, I) instead of HBF_4 originates the breaking of the paddlewheel structure of $[Rh_2(O_2CCH_3)_4]$ leading to RhX_3.[25,26]

The oxidation of the Rh_2^{4+} core to the Rh_2^{6+} unit to give $[Rh_2(O_2CCH_3)_4I_2]{\cdot}4H_2O$ (**4·4H$_2$O**) is only achieved when KI in neutral solution saturated with oxygen is used (procedure *c*). With KCl only the starting compounds were isolated and with KBr a mixture of the starting compounds and the compound **1·4H$_2$O** were isolated.

All attempts to oxidize the $[Rh_2(O_2CCH_3)_4]$ complex directly with I_2, Br_2 or Cl_2 failed. Although with Br_2 and Cl_2 some reaction occurs, we could not isolate the desired product; in these cases, only the formation of RhX_3 was detected. Moreover, the reaction of $[Rh_2(O_2CCH_3)_4]$ with O_2 in the absence of the halides, even in the presence of other counteranions (e.g. nitrate), does not produce the oxidation. Therefore, these data suggests that the equilibrium halide-oxygen could be the key of the oxidation process. In fact, it is well-known that KI solutions give iodine at pH $\leq$ 7, while KBr and KCl solutions only form bromine and chlorine at very acidic pH (Table S1 in the Supporting Information).

The IR spectra of complexes **1**–**4** show in the COO stretching region the typical pattern corresponding to the bridging carboxylato ligands. The υ_{as}(COO) absorption of the carboxylato group is shifted from 1568 cm^{-1} in the starting material to higher wavelengths for complexes **1**–**4**. The IR spectra of all complexes clearly show absorptions bands due to the presence of water molecules.

The structures of complexes **1**–**4** have been determined by single-crystal X-ray diffraction. Although the final data for compound **1·4H$_2$O** were not as good as the ones obtained for **2·4H$_2$O**, the structure has been included in the paper, because the data from the isostructural **2·4H$_2$O** allow us to support the proposed structure for **1·4H$_2$O**. Table 1 collects selected bond lengths and angles of the complexes.

The complexes **1·4H$_2$O** and **2·4H$_2$O** are isostructural, crystallizing in the same $P\bar{1}$ space group, with similar cell parameters. Figures 1 and 2 show the dimetallic unit and the counterion for both complexes. The anionic units $[Rh_2X(O_2CCH_3)_4]^-$ consist of two Rh atoms linked by four acetate bridging ligands in an eclipsed arrangement, with the axial positions occupied by one halide bridging ligand (Br^- and I^-, respectively), giving infinite *zig-zag* chains $(–Rh–Rh–X–)_x$ (X = Br, I) (Figure 3). Thus, each Rh atom shows a slightly distorted octahedral environment having four equatorial positions occupied by the oxygen atoms of the acetate ligands; the axial sites are occupied by one halide ligand and by the other Rh atom of the dimetallic unit. The Rh–Rh bond lengths in **1·4H$_2$O** and **2·4H$_2$O** are 2.3985(2) and 2.399(2) Å, respectively. These distances are consistent with those found in other carboxylatodirhodium complexes containing a Rh_2^{4+} unit.[1] The Rh–Br and Rh–I distances are 2.4014(12) and 2.7017(17) Å, in **1·4H$_2$O** and **2·4H$_2$O**, respectively.

Table 1. Selected bond lengths [Å] and angles [°] for compounds **1**–**4**.

	1·4H$_2$O	**2·4H$_2$O**	**3·H$_2$O**	**3·4H$_2$O**	**4·4H$_2$O**
Rh–Rh	2.398(1)	2.402(2)	2.3993(9)	2.3837(8)	2.413(1)
	2.401(1)	2.399(2)			
Rh(1)–O$_{(average)}$	2.041	2.045	2.029	2.038	2.049
Rh(2)–O$_{(average)}$	2.037	2.041			
Rh(1)–X	2.648(1)	2.701(2)	2.6828(5), 2.6827(5)	2.5321(5)	2.8852(1)
Rh(2)–X	2.645(1)	2.692(2)			
Rh(1)–Rh(1)–X	177.29(5)	177.70(8)	176.69(3)	177.73(3)	179.69(5)
Rh(2)–Rh(2)–X	177.40(5)	177.65(8)			
Rh–X-Rh	130.75(4)	131.40(6)	180.00(1)	180	
O(1)–Rh(1)–Rh(1)–O(2)	91.18	1.03	89.34	0.12	0.29
O(5)–Rh(2)–Rh(2)–O(6)	89.19	1.96			

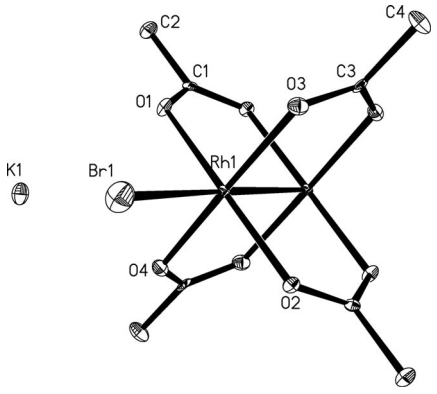

Figure 1. ORTEP view of one of the two binuclear units present in $K_x[Rh_2Br(O_2CCH_3)_4]_x \cdot 4xH_2O$ (**1·4H$_2$O**) complex showing the atom numbering scheme. Atoms are represented by thermal ellipsoids at the 50% probability level. Hydrogen atoms and solvation water molecules are omitted for clarity.

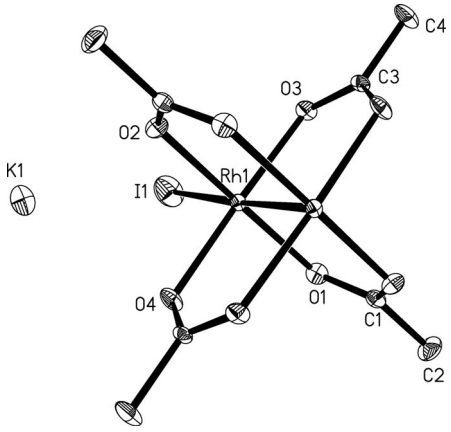

Figure 2. ORTEP view of one of two binuclear units present in $K_x[Rh_2I(O_2CCH_3)_4]_x \cdot 4xH_2O$ (**2·4H$_2$O**) complex showing the atom numbering scheme. Atoms are represented by thermal ellipsoids at the 30% probability level. Hydrogen atoms and solvation water molecules are omitted for clarity.

In the *zig-zag* chains the Rh–X–Rh angles are 130.75(4)° and 131.40(6)° in **1·4H$_2$O** and **2·4H$_2$O**, respectively. The disposition of chains is enhanced because the neighbouring pairs of $[Rh_2(O_2CCH_3)_4]$ units bridged by the halide ions are also supported by potassium cations along the chains.

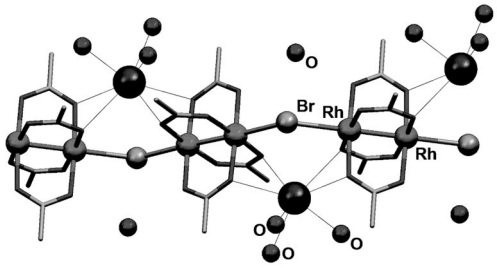

Figure 3. View of the chain structure of $K_x[Rh_2Br(O_2CCH_3)_4]_x \cdot 4xH_2O$ (**1·4H$_2$O**), showing interactions across the water molecules.

Thus, in both complexes each potassium ion is surrounded by seven oxygen atoms with distances ranging from 2.724 to 3.100 Å. Four oxygen atoms belong to carboxylato ligands (two of each neighbouring dimetallic units) and the other three belong to water molecules (Figure 3).

The *zig-zag* chains are held in parallel due to the hydrogen bonds formed by the four water molecules that hold the carboxylate oxygen atoms of adjacent dimetallic units with two water molecules in turn connected to potassium ions of different chains. The complex **2·4H$_2$O** shows very similar interactions.

To the best of our knowledge, complexes **1·4H$_2$O** and **2·4H$_2$O** represent the first reported examples of infinite chain structures of monohalotetracarboxylatodirhodium(II) complexes.[20,21,27]

The structure of the mixed-valence complexes **3·H$_2$O** and **3·4H$_2$O** consists of two Rh atoms linked by four acetate bridging groups with the axial positions occupied by chloride ligands (Figure 4 and Figure S1). The Rh–Rh distances are 2.3993(9) Å and 2.3837(8) for **3 H$_2$O** and **3·4H$_2$O**, respectively. These values lie in the range found in the Rh_2^{5+} compounds described in the literature (2.31–2.51 Å) and also in the range observed for dirhodium(II) species.[1] The small variation of the metal···metal distances in spite of the change in oxidation state agrees with the loss of one electron from a δ* orbital. Thus, the initial $\sigma^2\pi^4\delta^2\pi^{*4}\delta^{*2}$ configuration[28] for the reduced species change to $\sigma^2\pi^4\delta^2\pi^{*4}\delta^{*1}$ configuration for the mixed valence dirhodium(II,III) complexes. In contrast to the *zig-zag* chains observed for **1·4H$_2$O** and **2·4H$_2$O**, in **3·H$_2$O** and **3·4H$_2$O**, the $[Rh_2(O_2CCH_3)_4]^+$ units form linear chains. These linear

chains are also in contrast with the formation of *zig-zag* arrangements previously reported in the one-dimensional chains of $[Rh_2(acetamidato)X]_x$ complexes.[19–21]

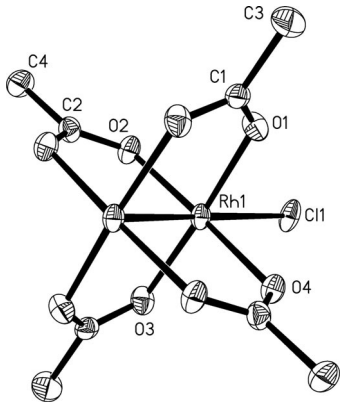

Figure 4. ORTEP view of the binuclear unit of complex **3·H_2O**, showing the atom numbering. Atoms are represented by thermal ellipsoids at the 30% probability level. Hydrogen atoms and solvation water molecules are omitted for clarity.

The interactions between the linear chains of $[Rh_2(O_2CCH_3)_4Cl]_x$ in both complexes occurs through interstitial water molecules. Thus, in complex **3·H_2O**, each water molecule connects, through several interactions, two perpendicular chains leading to a 3D arrangement in the solid state (Figure 5).

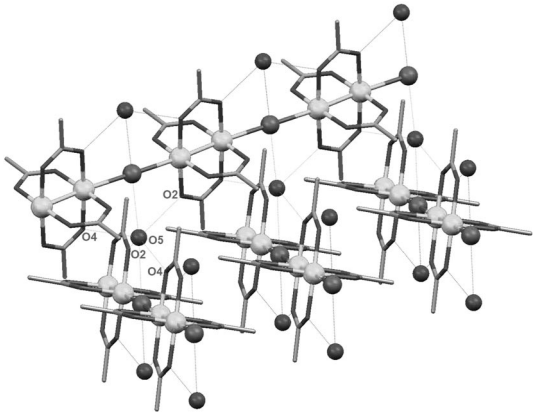

Figure 5. View of the chain structure of $[Rh_2(O_2CCH_3)_4Cl]_x \cdot H_2O$ (**3·H_2O**) showing interchain interactions.

In the case of complex **3·4H_2O**, the interactions take place among four chains through the oxygen atoms O5, O6, O7 in the way that depicts Figure 6, giving rise to a 3D arrangement.

Complexes **3·H_2O** and **3·4H_2O** constitute the first polymeric tetracarboxylatodirhodium(II,III) species described in the literature.

The structure of **4·H_2O** (Figure 7) consists of discrete dinuclear molecules of $[Rh_2(O_2CCH_3)_4I_2]$, with iodine atoms in the axial positions. The Rh–Rh distance [2.413(1) Å] lies in the range expected for the majority of tetracarboxylatodirhodium compounds (2.31–2.51 Å).[1] The Rh–Rh distances found in some previously described complexes containing the Rh_2^{6+} unit are larger than the distances observed in other species in lower oxidation states.[4e] This behaviour has been ascribed to the loss of the σ M–M interaction, leading to a $\pi^4\delta^2\pi^{*4}\delta^{*2}$ electronic configuration.[4e] However, the Rh–Rh distance in **4·4H_2O** is only slightly larger than the one found in complexes **1·4H_2O** and **2·4H_2O**, containing the Rh_2^{4+} unit, and also in **3·H_2O** and **3·4H_2O**, with the mixed valence core Rh_2^{5+}. This near invariability in the M–M distances could be consistent with the $\sigma^2\pi^4\delta^2\pi^{*4}$ electronic configuration. In addition, the eclipsed disposition of the paddlewheel unit is in accordance with the existence of a net δ bond in the dimetallic unit. Rh–I distance [2.8852(1) Å] is longer than in the polymeric complex **2·H_2O**. Similarly to that found in $Ru_2(DMBA)_4I_2$ complex[29] (DMBA = *N*,*N*′-dimethylbenzamidinate) the Rh–I distance in **4·4H_2O** is very close to the sum of the ionic radii of Rh^{3+} (0.67 Å) and I^- (2.20 Å) and much longer than the sum of the covalent radii of the elements. These data indicate that the nature of the Rh–I bonds in this complex is highly ionic.

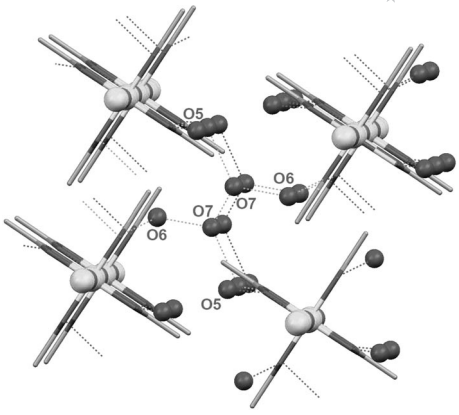

Figure 6. View of the chain structure of $[Rh_2(O_2CCH_3)_4Cl]_x \cdot 4xH_2O$ corresponding to complex **3·4H_2O**, showing the interactions between the water molecules.

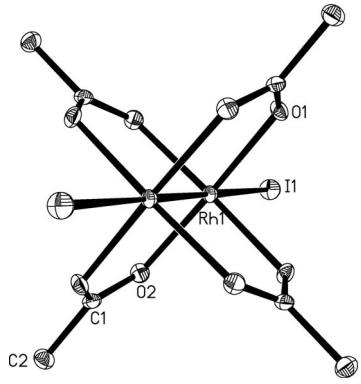

Figure 7. ORTEP view of the binuclear unit of complex $[Rh_2(O_2CCH_3)_4I_2] \cdot 4H_2O$ (**4·H_2O**) showing the atom numbering scheme. Atoms are represented by thermal ellipsoids at the 20% probability level. Hydrogen atoms and solvation water molecules are omitted for clarity.

The crystallization water molecules O4 and O6 are hydrogen bonded to an oxygen atom of the acetate ligand of the neighbouring dirhodium units [O4–O2 = 2.878(7) Å and O6–O1 = 2.968(9) Å]. These interactions generate a sheet parallel to the *ab* plane (Figure S2). The other two water molecules do not present any specific interaction.

Electrical conductivity of metal-organic compounds is a matter of current interest but still the number of compounds showing this physical property is very limited.[30] MMX and related systems seem to be suitable candidates to present electrical conductivity. Therefore, two probe direct current (DC) electrical conductivity measurements at 300 K were performed in several crystals of complexes **1·4H$_2$O**, **2·4H$_2$O** and **3·H$_2$O**. The conductivity values at 300 K applying an electrical current with voltages from +10 V to –10 V (Table 2) are in the range observed for other similar coordination polymers.

Table 2. Electrical conductivity data collected at 300 K for compounds **1·4H$_2$O**, **2·4H$_2$O** and **3·H$_2$O** compounds [$\sigma_{300\ K}$ (S cm^{-1})]. using the two probe technique.

Compounds	$\sigma_{300\ K}$ (S cm^{-1})
$[K(H_2O)_4]_x[Rh_2X(O_2CCH_3)_4]_x$ X = Br (**1·4H$_2$O**), I (**2·4H$_2$O**)	3.96×10^{-6}, 6.33×10^{-5}
$[Rh_2(O_2CCH_3)_4Cl]_x\cdot xH_2O$ (**3·H$_2$O**)	1.91×10^{-6}

Since compound **2·4H$_2$O** seems to be the best conductor, we have carried out more extended studies on this complex. Thus, DC-electrical conductivity measurements at variable temperature carried out by the standard four-probe method on the best developed face of a single crystal of **2·4H$_2$O** show a room temperature conductivity of ca. $2\cdot10^{-4}$ S cm^{-1}. Note that the factor of 3 between the two measurements may be attributed to the different measurement method and/or to the quality of the single crystals used. When the sample is cooled, the d.c. electrical resistivity smoothly increases from a value of ca. 5000 Ω cm at room temperature to a value of ca. 35000 Ω cm at ca. 60 K (Figure 8). Below this temperature the resistance of the crystal exceeded the limit of our measuring system. Interestingly, the thermal variation of the electrical resistivity does not follow the classical Arrhenius-type semiconducting regime (see inset in Figure 8), but rather a variable range hopping (VRH) model $\rho = \rho_0\times\exp(T_0/T)^{\alpha}$. This model reproduces very satisfactorily the resistivity of compound **2·4H$_2$O** in the whole temperature range with ρ_0 = 503(5) Ω cm, T_0 = 3739(79) K and α = 0.345(1) (solid line in Figure 8). The α value, very close to 1/3, indicates that the conductivity in this compound is essentially two dimensional. Although the structure of compound **2·4H$_2$O** is formed by *zig-zag* Rh–Rh–I chains, a close look at the structure shows the presence of one short interchain interaction between the I atom and one of the three water molecules bonded to the K cations. Thus, there is a I···O distance of 3.43 Å, shorter than the sum of the van der Waals radii of I and O (1.98 and 1.52 Å, respectively) (Figure 9). Additionally, there is a second short interchain interaction with an I···O distance of 3.61 Å. Interestingly, these interactions only take place in the *ac* plane but not in the *bc* plane, leading to a 2D structure formed by interconnected chains. Note that the oxygen atoms implied in these interactions correspond to water molecules and, therefore, the I···O interaction is expected to be mediated by the H atom in a I···H–O interaction.[31] Although these interactions are weak, the high polarizability and extension of the iodine orbitals is expected to facilitate the electron hopping observed in the plane.

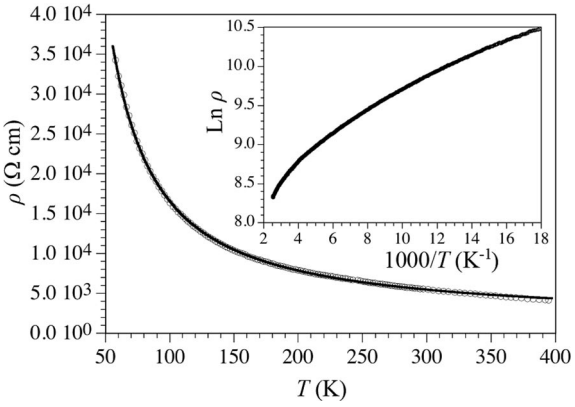

Figure 8. Thermal variation of the DC-resistivity of compound **2·4H$_2$O**. Solid line shows the best fit to the VRH model. Inset shows the corresponding Arrhenius plot.

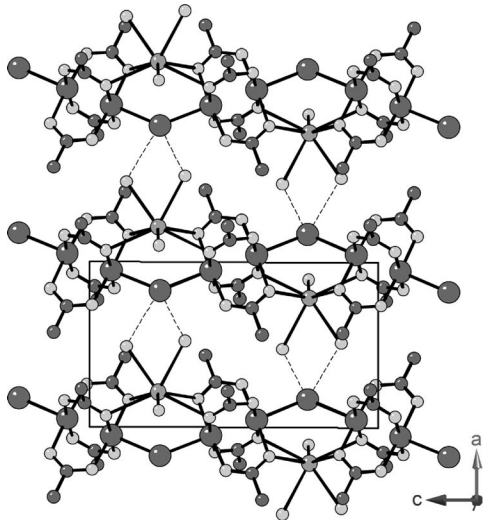

Figure 9. View of the chain structure of $K_x[Rh_2I(O_2CCH_3)_4]_x\cdot 4xH_2O$ (**2·4H$_2$O**) showing the interchain interactions in the *ac* plane.

It is worth noting that the number of conductivity studies on coordination polymers is scarce, particularly focusing on MMX polymers and specifically platinum and nickel mixed-valence compounds with dithiocarboxylato ligands (Table 3). In these cases the conductivity values of the complexes are between 83–6 10^{-4} S cm^{-1}. The data reported for dirhodium polymers are limited to three acetamidato

Table 3. Electrical conductivity data collected at 300 K for some selected MMX compounds [$\sigma_{300\,K}$ ($S\,cm^{-1}$), using the four probe technique].[32]

Compounds	σ 300 K ($S\,cm^{-1}$)
$[Pt_2(RCS_2)_4I]$	13 (R = Me), 5–30 (R = Et), 0.23 (R = *n*Pr), 17–83 (R = *n*Bu), 0.84 (R = *n*Pent)
$K_4[Pt(pop)_4Br]$ nH_2O (pop = diphosphito)	5×10^{-4}
$[Ni_2(RCS_2)_4I]$	2.5×10^{-2} (R = Me), 1.6 10^{-3} (R = Et), 7.6×10^{-4} (R = *n*Pr), 6 10^{-4} (R = *n*Bu)
$[Rh_2(CH_3NO_2)_4X]_x$ (X = Cl, Br, I)	2×10^{-7}

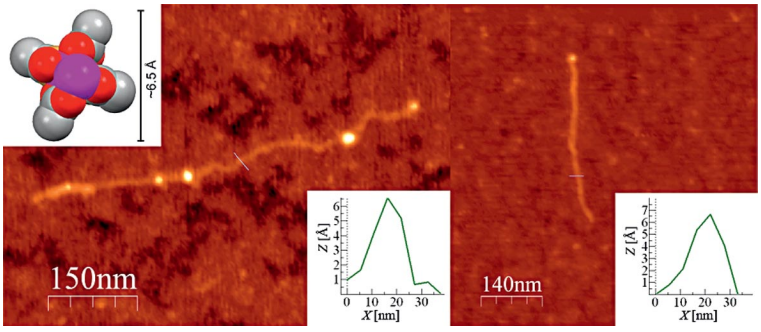

Figure 10. AFM topographic images of the fibres of complexes **1·4H$_2$O** (left) and **2·4H$_2$O** (right) adsorbed on mica.

mixed-valence (Rh_2^{5+}) complexes showing lower conductivity values than those observed for the acetate complexes (2×10^{-7} $S\,cm^{-1}$).[20,21] Surprisingly, in these polymers the conductivity values are almost equal and unaffected by the bridging halogen.

In addition, no conductivity studies of MMX without mixed-oxidation state have been made. Our results show that this kind of complexes can also present electrical conductivity at room temperature. The relatively high conductivity found in our compounds may be attributed to dispersions of the bands due to a high orbital overlap between the Rh^{2+} cations and the I^- anions along the chains as well as between the chains through the K^+ cations and the H-bonded water molecules.

The relatively high electrical conductivity values observed in the crystal phase for compounds **1·H$_2$O** and **2·H$_2$O** prompted us to consider these materials as a suitable candidate towards molecular wires formation on surface. Therefore, the first necessary requirement is the characterization on surfaces of isolated single chains or nanostructures of these materials. Recent studies have developed routes of isolation for these types of systems on surfaces.[33,34] Following a similar methodology already reported by us for MMX chains of ruthenium, we have carried out the adsorption of **1·H$_2$O** and **2·H$_2$O** on mica. The deposition of sonicated water diluted solutions of these compounds on mica, allows isolation of individual chains whose morphological characterization has been performed by atomic force microscopy (AFM)[33] confirming the isolation of 1D organizations. Figure 10 shows AFM topography images of homogeneous fibres (complexes **1·4H$_2$O** and **2·4H$_2$O**) obtained upon standing several days (4 days for **1·4H$_2$O**, 6 days for **2·4H$_2$O**) from sonicated solution at room temperature. The height values of ca. 0.6 nm obtained in both cases are in good agreement with the values of the diameters observed by X-ray diffraction for individual polymer chains.

Conclusions

The scarce synthetic routes previously reported used to prepare dirhodium(II,III) and dirhodium(III) complexes are somehow complicated and specific, involving inert atmospheres and ultra-dried solvents. Therefore, the oxidation reaction of tetraacetatodirhodium(II) using oxygen, in aqueous solution with pH control, constitutes a very interesting and suitable method to obtain tetraacetatodirhodium(II,III) and (III,III) complexes. This simple procedure has allowed us to prepare linear and *zig-zag* chain polymers, containing tetraacetatodirhodium units, with electrical conductivity. Isolation and AFM characterization on surface of these polymers point out the potential of these materials as molecular wires.

The preliminary data herein presented suggest that this synthetic approach could be employed for the preparation of other similar dirhodium carboxylate complexes. Work is underway to explore the structural scope and applications of these new complexes.

Experimental Section

General Procedures: KBr, $RhCl_3{\cdot}xH_2O$, carboxylic acids, and solvents were purchased and used as received. The tetraacetatodirhodium(II) used in this report was obtained by a method described before.[34,35] IR spectra were recorded on a PerkinElmer Spec-

trum 100 spectrophotometer using an universal ATR sampling accessory. Elemental Analyses were carried out by the Microanalytical Service of the Complutense University of Madrid.

Preliminary direct current (DC) electrical conductivity measurements were performed on two different single crystals of compounds **1·4H$_2$O**, **2·4H$_2$O** and **3·H$_2$O** at 300 K with two contacts. The contacts were made with platinum wires (25 μm diameter). The samples were measured at 300 K applying an electrical current with voltages form +10 to –10 V. The measurements were performed in the compounds along the crystallographic *a* axis. Variable temperature DC-resistivity measurements were performed with the four contacts method on a single crystal of compound **2·4H$_2$O** in the temperature range 60–400 K. The contacts were made with platinum wires (25 μm of diameter) that were attached to the crystals with graphite paint. The measurements were performed with a current intensity of 10 nA at a scan rate of 0.5 K/min with reproducible and very similar results in the cooling and warming scans. The resistivity measurements were done with a Quantum Design Physical Properties Measurement System (PPMS-9) equipment.

X-ray Data Collection and Structure Refinement: Data collection for all compounds was carried out at room temperature on a Bruker Smart CCD diffractometer using graphite-monochromated Mo-K_α radiation (λ = 0.71073 Å) operating at 50 kV for all compounds and 20 mA for **1·4H$_2$O** and **2·4H$_2$O** and 30 mA for **3·H$_2$O**, **3·4H$_2$O** and **4·4H$_2$O**. In all cases, data were collected over a hemisphere of the reciprocal space by combination of three exposure sets. Each exposure of 20 s covered 0.3 in ω. Cell parameters were determined and refined by a least-squares fit of all reflections. The first 100 frames were recollected at the end of the data collection to monitor crystal decay, and no appreciable decay was observed. A semi-empirical adsorption correction was applied for all cases. The crystal structure of complex **1·4H$_2$O** has not been refined satisfactorily due to the low quality of the crystal. However, as compound **1·4H$_2$O** is isostructural with **2·4H$_2$O**, we have included the structure of the former to explain the structure-properties relationship in this compound.

A summary of the fundamental crystal and refinement data is given in Table 4.

The structures were solved by direct methods and refined by full-matrix least-square procedures on F^2 (SHELXL-97).[36] All non-hydrogen atoms were refined anisotropically. For all compounds the Fourier difference map showed, in the last cycles of refinement, residual electronic density, that was assigned to the oxygen atoms of solvent water molecules. However, the corresponding hydrogen atoms could not be located and were not included in the model. The rest of the hydrogen atoms were included in their calculated positions and refined riding on the respective carbon atoms.

CCDC-775468 (for **1·4H$_2$O**), -775469 (for **2·4H$_2$O**), -775470 (for **3·H$_2$O**), -775471 (for **3·4H$_2$O**), -775472 (for **4·4H$_2$O**) contain the supplementary crystallographic data for this paper. These data can be obtained free of charge from The Cambridge Crystallographic Data Centre via www.ccdc.cam.ac.uk/data_request/cif.

Atomic Force Microscopy (AFM): Atomic Force Microscopy images were acquired in dynamic mode using a Nanoscope IIIa Multimode Veeco Electronica System. Veeco cantilevers were used with a nominal force constant of 0.75 N/m operating at room temperature under ambient air conditions. The images were processed using WSxM[37] (freely downloadable SPM software from www.nanotec.es).

Preparation of the Surfaces: To obtain reproducible results, very flat surfaces with precisely controlled chemical functionalities, freshly prepared just before the chemical deposition, were used. The commercially available (Telstar) support used was Muscovite Mica. Before the chemical deposition, the mica surfaces were cleaved with an adhesive tape.

Sample Preparation: 3 mg of $K_x[Rh_2X(O_2CCH_3)_4]_x{\cdot}4xH_2O$ (X = Br and I), were suspended in 1 mL of H_2O and sonicated in a

Table 4. Crystal and refinement data for: **1·4H$_2$O**, **2·4H$_2$O**, **3·H$_2$O**, **3·4H$_2$O**, and **4·4H$_2$O**.

	1·4H$_2$O	**2·4H$_2$O**	**3·H$_2$O**	**3·4H$_2$O**	**4·4H$_2$O**
Formula	$C_8H_{20}BrKO_{12}Rh_2$	$C_8H_{20}IKO_{12}Rh_2$	$C_8H_{14}ClO_9Rh_2$	$C_8H_{20}ClO_{12}Rh_2$	$C_8H_{20}I_2O_{12}Rh_2$.
Mr	625.01	672.00	493.45	585.54	887.80
Crystal system	triclinic	triclinic	monoclinic	triclinic	orthorhombic
Space group	$P\bar{1}$	$P\bar{1}$	*C*2/*c*	$P\bar{1}$	*Ibam*
a [Å]	7.9837(8)	8.080(4)	9.291(1)	7.4465(9)	14.7511(8)
b [Å]	8.0129(8)	8.1072(4)	12.437(1)	8.057(1)	12.2791(7)
c [Å]	14.068(1)	14.2736(7)	12.326(1)	8.965(2)	13.7736(8)
α [°]	83.838(4)	83.705(1)	–	85.907(2)	–
β [°]	89.265(4)	89.355(1)	97.069(2)	82.655(2)	–
γ [°]	87.135(4)	87.096(1)	–	67.652(2)	–
V [Å^3]	893.6(2)	928.21(8)	1413.4(3)	493.2(1)	2494.8(2)
Z	2	2	4	1	4
F(000)	600	636	956	291	1664
D(calcd.) [g cm^{-3}]	2.323	2.404	2.319	1.972	2.364
μ [mm^{-1}]	4.369	3.717	2.561	1.869	3.878
Scan technique	ω and ϕ	ω and ϕ	ω and ϕ	ω and ϕ	ω and ϕ
Data collected	(–9, –9, –16) to (9,8,16)	(–9, –9, –16) to (8,8,16)	(–11, –15, –12) to (11,15,15)	(–8, –7, –10) to (8,9,10)	(–18, –15, –17) to (17,15,17)
θ°	1.46 to 25.00	1.44 to 25.01	2.75 to 27.00	2.29 to 25.01	2.16 to 26.98
Reflections collected	13576	7167	6126	3809	10714
Independent reflections	3090 (R_{int} = 0.0417)	3178 (R_{int} = 0.0215)	1539 (R_{int} = 0.0429)	1693 (R_{int} = 0.0261)	1423 (R_{int} = 0.0285)
Data/restraints/parameters	3090/0/217	3178/0/217	1539/0/93	1693/0/115	1423/0/78
Obsd. reflections [$I > 2\sigma(I)$]	2919	2846	1171	1413	1284
R[a]	0.0664	0.0766	0.0403	0.0324	0.0376
Rw_F[b]	0.1852	0.2490	0.1149	0.0845	0.1347

[a] $R = \Sigma||F_o| - |F_c||/\Sigma|F_o|$. [b] $Rw_F = \{\Sigma[w(F_o^2 - F_c^2)^2]/\Sigma[w(F_o^2)^2]\}^{1/2}$.

ultrasounds probe at 680 W for 2 h at 40 °C Then, the dispersions of **1·4H$_2$O** and **2·4H$_2$O** in water were obtained and diluted to a concentration of 3 10^{-6} mg/mL and 20 μL of the diluted solutions were deposited on mica upon different standing times. Fibre formation was observed for **1·4H$_2$O** and **2·4H$_2$O** after a period of 4 and 6 d, respectively.

K$_x$[Rh$_2$Br(O$_2$CCH$_3$)$_4$]$_x$·4xH$_2$O (1·4H$_2$O): To a water solution (15 mL) of tetraacetatodirhodium(II) (0.100 g, 0.226 mmol), 0.027 g, (0.226 mmol) of KBr was added (pH = 6.5). The suspension was stirred for 12 h at 25 °C and then filtered off.

Clear green crystals were obtained by slow evaporation at room temperature; yield 31 mg (22.3%). The compound can be manipulated in air without appreciable decomposition for a long period of time. $C_8H_{20}BrKO_{12}Rh_2$ (633.06): calcd. C 15.35, H 3.20; found C 15.62, H 2.95. IR: ṽ = 3539 (m), 3489 (m), 3413 (m), 3276 (m), 1646 (m), 1577 (s), 1412 (vs), 1354 (m), 1042 (m), 700 (s) cm^{-1}.

K$_x$[Rh$_2$I(O$_2$CCH$_3$)$_4$]$_x$·4xH$_2$O (2·4H$_2$O): To a water solution (15 mL.) of tetraacetatodirhodium(II) (0.100 g, 0.226 mmol), 0.037 g, (0.226 mmol) of KI was added (pH = 6.7). The suspension was stirred for 12 h at 25 °C and then filtered off. Clear green crystals were obtained by slow evaporation at room temperature; yield 35 mg (23.3%). The compound can be manipulated in air without appreciable decomposition for a long period of time. $C_8H_{20}IKO_{12}Rh_2$ (680.06): calcd. C 14.28, H 2.98; found C 14.64, H 2.71. IR: ṽ = 3412 (br. m), 1637 (m), 1579 (s), 1411 (vs), 1350 (m), 1080 (br. s), 1046 (br. s) 700(s) cm^{-1}.

[Rh$_2$(O$_2$CCH$_3$)$_4$Cl]$_x$·xH$_2$O (3·H$_2$O): To a water solution (15 mL) of tetraacetatodirhodium(II) (0.085 g, 0.192 mmol) saturated with O_2, 0.015 g, (0.171 mmol) of HBF_4 and 0.008 g, (0.171 mmol) of KCl were added (pH = 1.5). The suspension was stirred for 24 h at 25 °C and then filtered off. Clear green crystals were obtained by slow evaporation at room temperature; yield 4 mg (4%). The compound can be manipulated in air without appreciable decomposition for a long period of time. $C_8H_{14}ClO_9Rh_2$ (495.46): calcd. C 19.45, H 2.84; found C 19.41, H 2.79. IR: ṽ = 3464 (br. m), 1631 (w), 1577 (s), 1439 (sh), 1412 (vs), 1348 (m), 1046 (w), 1029 (w) 702(s) cm^{-1}.

[Rh$_2$(O$_2$CCH$_3$)$_4$Cl]$_x$·4xH$_2$O (3·4H$_2$O): To a water solution (15 mL) of tetraacetatodirhodium(II) (0.05 g, 0.113 mmol) saturated with O_2, 0.006 g, (0.113 mmol) of NH_4Cl and 0.003 g (0.018 mmol) of $CuCl_2·2H_2O$ were added (pH = 4.6). The suspension was stirred for 24 h at 25 °C and then filtered off. Clear green crystals were obtained by slow evaporation at room temperature; yield 6 mg (10%). The compound can be manipulated in air without appreciable decomposition for a long period of time. $C_8H_{20}ClO_{12}Rh_2$ (549.50): calcd. C 16.39, H 3.41; found C 16.41, H 2.79. IR: ṽ = 3466 (br. m), 1631 (w), 1578 (s), 1436 (sh), 1408 (vs), 1348 (m), 1044 (w), 700 (s) cm^{-1}.

[Rh$_2$(O$_2$CCH$_3$)$_4$I$_2$]·4H$_2$O (4·4H$_2$O): To a water solution (15 mL.) of tetraacetatodirhodium(II) (0.100 g, 0.226 mmol) saturated with O_2 (pH = 6.7), 0.075 g, (0.452 mmol) of KI was added. The suspension was stirred for 12 h at 25 °C and then filtered off. Clear green crystals were obtained by slow evaporation of the filtrate at room temperature; yield 30 mg (17.3%). The compound can be manipulated in air without appreciable decomposition for a long period of time. $C_8H_{20}I_2O_{12}Rh_2$ (767.86): calcd. C 10.82, H 1.36; found C 10.64, H 1.83. IR: ṽ = 3554 (m), 3497 (m), 3407 (m), 1644 (m), 1574 (s), 1413 (s), 1350 (m), 1046 (m), 703 (s) cm^{-1}.

Supporting Information (see also the footnote on the first page of this article) collects an ORTEP view of the binuclear unit of complex **3·4H$_2$O**, the hydrogen bond interactions in the **4·4H$_2$O** compound, and potential of the halide oxidation by oxygen at different pH values.

Acknowledgments

We are grateful to the Ministerio de Ciencia e Innovación (MCINN) (Projects no. CTQ2008-00920, MAT2007-61584 and CSD2007-00010, Consolider-Ingenio in Molecular Nanoscience), the European Union (MAGMANet), the Comunidad de Madrid (project no. S2009/MAT-1467), the Generalitat Valenciana (Project no. PROMETEO/2009/095) and Banco Santander Central Hispano – Universidad Complutense de Madrid (BSCH-UCM-921073-4120824) for financial support. Ana Soubrie is thanked for her valuable help with AFM measurements.

[1] F. A. Cotton, C. A. Murillo, R. A. Walton, in: *Multiple Bonds Between Metal Atoms*, 3rd ed. (Eds.: F. A. Cotton, A. Murillo, R. A. Walton), 3rd ed., Springer Science and Business Media, Inc., New York, **2005**, p. 465–590.

[2] See, for example, some recent papers: a) E. R. Milaeva, N. N. Meleshonkova, D. B. Shpakovsky, K. V. Uspensky, A. V. Dolganov, T. V. Magdesieva, A. V. Fionov, A. A. Sidorov, G. G. Aleksandrov, I. L. Eremenko, *Inorg. Chim. Acta* **2010**, *363*, 1455–1461; b) L. E. Joyce, J. D. Aguirre, A. M. Angeles-Boza, A. Chouai, P. K.-L. Fu, K. R. Dunbar, C. Turro, *Inorg. Chem.* **2010**, *49*, 5371–5376; c) Y. Watanabe, T. Washio, N. Shimada, M. Anada, S. Hashimoto, *Chem. Commun.* **2009**, 7294–7296; d) D. V. Deubel, *J. Am. Chem. Soc.* **2008**, *130*, 665–675; e) J. Hansen, H. M. L. Davies, *Coord. Chem. Rev.* **2008**, *252*, 545–555; f) H. T. Chifotides, K. R. Dunbar, *Chem. Eur. J.* **2008**, *14*, 9902–9913; g) S. J. Na, B. Y. Lee, N.-N. Bui, S. Mho, H.-Y. Jang, *J. Organomet. Chem.* **2007**, *692*, 5523–5527; h) E. Galdecka, Z. Galdecki, F. P. Pruchnik, R. Starosta, *Trans. Met. Chem.* **1999**, *24*, 100–1003.

[3] See, for example: a) J. L. Bear, B. Han, Y. Li, S. Ngubane, E. Van Caemelbecke, K. M. Kadish, *Polyhedron* **2009**, *28*, 1551–1555, and references cited therein; b) Z. Yang, M. Ebihara, T. Kawamura, *Inorg. Chim. Acta* **2006**, *359*, 2465–2471; c) J. F. Berry, F. A. Cotton, P. Huang, C. A. Murillo, X. Wang, *Dalton Trans.* **2005**, 3713–3715.

[4] a) J.-H. Xie, L. Zhou, C. Lubek, M. P. Doyle, *Dalton Trans.* **2009**, 2871–2877; b) J.-H. Xie, M. P. Doyle, *J. Mex. Chem. Soc.* **2009**, *53*, 143–146; c) J.-H. Xie, J. M. Nichols, C. Lubek, M. P. Doyle, *Chem. Commun.* **2008**, 2671–2673; d) J. Wolf, R. Poli, J.-H. Xie, J. Nichols, B. Xi, P. Zavalij, M. P. Doyle, *Organometallics* **2008**, *27*, 5836–5845; e) J. M. Nichols, J. Wolf, P. Zavalij, B. Varughese, M. P. Doyle, *J. Am. Chem. Soc.* **2007**, *129*, 3504–3505.

[5] S. A. Hilderbrand, M. L. Lim, S. J. Lippard, *J. Am. Chem. Soc.* **2004**, *126*, 4972–4978.

[6] J. K. Bera, K. R. Dunbar, *Angew. Chem. Int. Ed.* **2002**, *41*, 4453–4457.

[7] A. K. Mahapatro, J. Ying, T. Ren, D. B. Janes, *Nano Lett.* **2008**, *8*, 2131–2136.

[8] B. Xi, T. Ren, *C. R. Chim.* **2009**, *12*, 321–331.

[9] K. R. Mann, M. J. DiPierro, T. P. Gill, *J. Am. Chem. Soc.* **1980**, *102*, 3965–3967.

[10] V. M. Miskowski, I. S. Sigal, K. R. Mann, H. B. Gray, S. J. Milder, G. S. Hammond, P. R. Ryason, *J. Am. Chem. Soc.* **1979**, *101*, 4383–4385.

[11] I. S. Sigal, K. R. Mann, H. B. Gray, *J. Am. Chem. Soc.* **1980**, *102*, 7252–7256.

[12] M. O. Albers, D. J. Robinson, N. J. Coville, *Coord. Chem. Rev.* **1986**, *69*, 127–258.

[13] T. R. Felthouse, *Prog. Inorg. Chem.* **1982**, *29*, 73–166.

[14] C. C. Tejel, A. Miguel, L. A. Oro, *Chem. Eur. J.* **1999**, *5*, 1131–1135.

[15] H. Kitagawa, N. Onodera, T. Sonoyama, M. Yamamoto, T. Fukawa, T. Mitani, M. Seto, Y. Maeda, *J. Am. Chem. Soc.* **1999**, *121*, 10068–10080.
[16] T. M. Minoru Mitsumi, H. Kishida, T. Yoshinari, K. T. Yoshiki Ozawa, T. Sonoyama, H. Kitagawa, T. Mitani, *J. Am. Chem. Soc.* **2001**, *123*, 11179–11192.
[17] K. S. Satoaki Ikeuchi, Y. Nakazawa, M. Mitsumi, M. S. Koshiro Toriumi, *J. Phys. Chem. B* **2004**, *108*, 387–392.
[18] L. Welte, R. Di Felice, F. Zamora, J. Gómez-Herrero, *Nat. Nanotechnol.* **2010**, *5*, 110–115.
[19] Y. Takazaki, Z. Yang, M. Ebihara, K. Inoue, T. Kawamura, *Chem. Lett.* **2003**, *32*, 120–121.
[20] Z. Yang, M. Ebihara, T. Kawamura, T. Okubo, T. Mitani, *Inorg. Chim. Acta* **2001**, *321*, 97–106.
[21] Z. Yang, T. Fujinami, M. Ebihara, K. Nakajima Kitagawa, T. H. Kawamura, *Chem. Lett.* **2000**, 1006–1007.
[22] S. Delgado, P. J. Sanz Miguel, J. L. Priego, R. Jiménez-Aparicio, C. J. Gómez-García, F. Zamora, *Inorg. Chem.* **2008**, *47*, 9128–9130.
[23] L. Welte, E. Mateo-Martí, P. Amo-Ochoa, P. J. Sanz Miguel, J. Gómez-Herrero, J. A. Martín-Gago, F. Zamora, *Chem. Commun.* **2008**, 945–947.
[24] P. Amo-Ochoa, S. S. Alexandre, L. Welte, P. J. de Pablo, M. I. Rodríguez-Tapiador, J. Gómez-Herrero, F. Zamora, *Inorg. Chem.* **2009**, *48*, 7931–7936.
[25] H. D. Glicksman, A. D. Hamer, T. J. Smith, R. A. Walton, *Inorg. Chem.* **1976**, *15*, 2205–2209.
[26] H. D. Glicksman, R. A. Walton, *Inorg. Chim. Acta* **1979**, *33*, 255–259.
[27] F. A. Cotton, M. A. Petrukhina, *Angew. Chem. Int. Ed.* **2000**, *39*, 2362–2364.
[28] J. G. Norman, G. E. Renzoni, D. A. Case, *J. Am. Chem. Soc.* **1979**, *101*, 5256–5267.
[29] W.-Z. Chen, T. Ren, *Inorg. Chem.* **2003**, *42*, 8847–8852.
[30] R. Mas-Ballesté, O. Castillo, P. J. S. Miguel, D. Olea, J. Gómez-Herrero, F. Zamora, *Eur. J. Inorg. Chem.* **2009**, 2885–2896.
[31] T. Steiner, *Angew. Chem. Int. Ed.* **2002**, *41*, 48–76.
[32] M. Mitsumi, T. Murase, H. Kishida, T. Yoshinari, Y. Ozawa, K. Toriumi, T. Sonoyama, H. Kitagawa, T. Mitani, *J. Am. Chem. Soc.* **2001**, *123*, 11179–11192.
[33] P. Amo-Ochoa, M. I. Rodríguez-Tapiador, O. Castillo, D. Olea, A. Guijarro, S. S. Alexandre, J. Gómez-Herrero, F. Zamora, *Inorg. Chem.* **2006**, *45*, 7642–7650.
[34] D. Olea, S. S. Alexandre, P. Amo-Ochoa, A. Guijarro, F. de Jesús, J. M. Soler, P. J. de Pablo, F. Zamora, J. Gómez-Herrero, *Adv. Mater.* **2005**, *17*, 1761–1765.
[35] G. A. Rempel, P. Legzdins, H. Smith, G. Wilkinson, *Inorg. Synth.* **1972**, 90–91.
[36] G. M. Sheldrick, *Program for Refinement of Crystal Structure*, University of Göttingen, Göttingen, Germany **1997**.
[37] R. F. I. Horcas, J. M. Gómez-Rodríguez, J. Colchero, J. Gómez-Herrero, A. M. Baro, *Rev. Sci. Instrum.* **2007**, *78*, 013705.

Received: July 6, 2010
Published Online: September 15, 2010

